Cranial trauma in handgun executions

Title: Cranial trauma in handgun executions: Experimental Data Using Polyurethane Proxies

Authors: Seth Taylor, Elena F. Kranioti

PII: S0379-0738(17)30490-5
DOI: https://doi.org/10.1016/j.forsciint.2017.11.032
Reference: FSI 9076

To appear in: *FSI*

Received date: 1-8-2017
Revised date: 16-11-2017
Accepted date: 20-11-2017

Please cite this article as: Seth Taylor, Elena F.Kranioti, Cranial trauma in handgun executions: Experimental Data Using Polyurethane Proxies, Forensic Science International https://doi.org/10.1016/j.forsciint.2017.11.032

Cranial trauma in handgun executions: Experimental Data Using Polyurethane Proxies

Seth Taylor[1], Elena F. Kranioti[1,2]

[1]Edinburgh Unit of Forensic Anthropology, School of History, Classics and Archaeology, University of Edinburgh, Edinburgh, UK.

[3]Forensic Pathology Division Crete, Hellenic Republic Ministry of Justice Transparency and Human Rights, Heraklion, Crete, Greece.

Author of correspondence and reprint requests

* Elena F. Kranioti, M.D., Ph.D.
Edinburgh Unit of Forensic Anthropology, University of Edinburgh
Old Medical School, Teviot Place, EH8 9AG, Edinburgh, UK
Tel. +44 (0)131 6502368
Email: elena.kranioti@ed.ac.uk

Highlights

- Ballistic trauma is often a critical subject of forensic investigations.
- PBS spheres are proven to be a reliable proxy for the cranial vault
- Experiments were done to simulate close range simulated executions.
- The size of the entrance wound is positively correlated with the caliber dimension
- Endocranial beveling increased with muzzle velocity but not with bullet weight

Abstract

Gun violence is a global phenomenon with regional variation in frequency and severity. Handguns are often used in violent deaths such as suicides and homicides. Hence, ballistic trauma is a critical subject of forensic investigations. Trauma patterns are fundamental evidence for the reconstruction of the incident and for the determination of the manner of death. This study investigated the differences in trauma patterns with a series of experiments using six different calibers (.22 LR, .38 Special, .380 ACP, 9 x 19 mm, .40 S&W, and .45 ACP) and four different bullet types. Synbone® spheres (polyurethane bone proxies) were used for close range 30 centimeter (cm) simulated executions. The polyurethane spheres constitute an excellent proxy for human crania at the macroscopic level as suggested

by other studies. The results showed that the radius of the entrance wound is positively correlated (Pearson's correlation coefficient R=0.846, $p<0.05$) with the caliber dimension. As muzzle velocity increased, endocranial beveling increased. Bullet weight, conversely, does not seem to have an effect on the size of the endocranial beveling present in Synbone® spheres. The ballistic experiments exhibited similarities in entrance wound morphology; radial and concentric fracture patterns, hydraulic burst effect, circumferential delamination, and endocranial beveling with that of documented forensic cases with corresponding caliber shot. Synbone spheres seem appropriate for ballistic simulations of cranial injuries; yet, more research is needed to verify these observations.

Keywords: Gunshot wound, ballistics, cranial trauma, polyurethane spheres, Synbone, execution

Introduction

Gun violence associated with civilian crime is a global problem. The magnitude of gun used in crime differs by country and or by region. According to a recent analysis of violent deaths in 24 high-income countries for 2010 [1] the firearm homicide rate was 25 times higher in the United States than in other high-income countries. More specifically, the average rate of gun related homicides per 100,000 habitants was 3.6 for the US [1] while in Europe the highest rates were recorded for Montenegro (1.87), Cyprus (1.28) and FYROM (1.02) [2]. European frequency of gun ownership ranges from 0.7 to 45.7 guns per 100 habitants while handgun ownership peaks (77%) in Germany [2]. The type of gun and ammunition is highly associated with the inflicted injuries in fatal assaults and the injury patterns comprise explicit markers for the differentiation between suicides, accidental deaths and homicides with firearms [3-5]. This study proposes an experimental setting to investigate the relationship between handgun and ammunition type and the inflicted injuries on a human skull under controlled conditions. Our aim is to assist future gunfire-related forensic investigations, as scientists attempt to determine the make of bullets used in deadly shooting events from close range.

There are two main types of fractures associated with gunshot wounds - radiating and concentric - which can form if the kinetic energy of the projectile is high enough. Radiating fractures diffuse away from the area of impact while concentric fractures form perpendicular to radiating fractures, giving the wound a spider web appearance [3-7]. Due to the anatomy of the skull, fractures occur in areas that are structurally weaker [5]. Radiating fractures emanating from the point of ballistic contact will follow the path of least resistance and cease when they intersect a previous fracture (Puppe's Rule) [3-5, 8,]. Factors such as the type of weapon, muzzle distance, and angle from the target can greatly affect the appearance of the cranial trauma and obscure the circumstances of the traumatic event [4-5]. With this in mind, reconstructing the shooting event by considering these factors can contextualize the incident. Investigating the range of variability of how the shooting event unfolded through experimental settings, can aid in interpreting violent homicidal shooting deaths. In fact, ballistic testing has been proposed as best practice many decades ago as described by Moritz in his 1954 publication [3].

Polyurethane bone substitute (PBS) spheres have been recently introduced in ballistic testing. Mechanically, they are considered a good proxy for human crania because they fracture with similar patterns. A detailed assessment of this can be found in Thali et al. [11-13]. Their experiments investigated fracture patterns on PBS spheres caused by contact and distance shots (10 meters) with a 9 x 19 millimeter (mm) Full Metal Jacket (FMJ). They concluded that the fracture patterns seen on PBS spheres were similar to cranial fractures resulting from ballistic injuries. More specifically, the entrance and exit wounds of the PBS spheres, the fracture lines, and the endocranial beveling of the entrance and exit wounds were similar to what occurs in cranial bone assessed from forensic cases. These studies suggest that the PBS spheres were well suited for ballistic testing [11-13]. This is supported by other studies investigating other types of blunt force injuries [10; 14-15].

Expanding on Thali et al. [11-13], Smith et al. [16], studied the micro and macroscopic differences and similarities of Synbone® PBS spheres as a proxy to human crania using four different weapons. Their research used a black powder .58 caliber muzzle loader, a 7.62 x 51 mm NATO (North Atlantic Treaty Organization), a .243 soft point hunting round, and a crossbow bolt. There is detailed literature on the effects of microfracture patterns with high-

velocity rifle ammunition and the distinguishable features between different types of high-velocity rifle rounds [17]. Smith et al. [16] found the PBS spheres to be a poor proxy at the microscopic level compared to the encouraging results from the macroscopic observation of trauma following their ballistic experiments. It must be acknowledged though that their sample was very small to draw any definite conclusions.

Fractures associated with ballistic trauma are extremely important in establishing the cause and manner of death in Gun Shot Wounds (GSW) incidents. Often fracture patterns seen in bone can help support or diminish testimony by suspects or eyewitnesses. Controlled experimental settings used to test assumptions about bullet caliber size and fractures patterns will help in determining these scenarios. In our study, Synbone® spheres were considered to be an excellent proxy for close range simulated executions targeting the cranial vault. The selection of PBS spheres filled with ballistic gelatin is in accordance with published studies reporting that these constitute a reliable proxy for macroscopic observations [11-16]. In addition, Synbone® ballistic spheres are an ethical and inexpensive proxy for human crania to conduct macroscopic ballistic testing [16] and are preferable compared to animal models. The purpose of this study is to explore the fracture characteristics of simulated head trauma provoked by different handguns, calibers, and ammunition types and its significance in weapon identification while the distance and direction of the shot to the target, as well as the anatomical region of infliction, remain controlled.

2. Materials and Methods

2.1 Materials

Synbone®

This study utilized Synbone® ballistic spheres as a proxy for human crania. Synbone® is a polyurethane synthetic bone material used for ballistic proxies. Synbone® has many different sphere types. Measurements from human cranial bones returned thicknesses that fall into the 5 mm range for the frontal, parietal, and occipital bones [18-19]; hence for this study, 5 mm ballistic spheres with a latex layer simulating periosteum were used [20]. These spheres are constructed of two hemispheres and glued together

simulating a 360-degree continuous suture around the sphere. There is a 4 cm diameter hole at the bottom of the sphere simulating a foramen magnum, from which the spheres are filled with ballistic gelatin to simulate a human brain. Fluka, Type 3, porcine gelatin, mixed with 360 grams (gm) of ballistic powder to 3.2 liters of water per sphere was chilled at 4 degrees Celsius for twenty-four hours.

Medium Velocity Impacts

This study utilized six different handgun calibers: .22 Long Rifle (LR), .38 Special, .380 Automatic Colt Pistol (ACP), 9 x 19 mm, .40 Smith & Wesson (S&W), and .45 ACP. All rounds fired in this study are considered medium velocity. Medium velocity rounds fall between 152 m/s to 457 m/s [21-23] Table 1.

Bullet Design

This study used two types of bullets: round nose and flat nose. The round nose bullet has a rounded nose of the bullet tip. The .22 LR, .380 ACP, 9 x 19mm, and .45 ACP were all round nose bullets. A flat nose is a round nose bullet in appearance and function with a flat tip. The .38 Special and .40 S&W were flat nose. Figure 1 illustrates all ammunition types used in this study.

2.2 Methods

The Shooting Range

The National Shooting Range, Chania, located at 73100 Kambani, Chania, Greece was used for the experiments. The range consists of outdoor trap/skeet shooting ranges, outdoor rifle ranges and outdoor pistol ranges. The live fire iterations were conducted on the private firing line.

Experimental Setting

The experiments were undertaken to determine the effectiveness of Synbone® spheres filled with ballistic gelatin to simulate brain matter as a proxy to human skulls during ballistic trials of six different pistol calibers shot in an execution style to recreate the recent militant executions. All Synbone® spheres were shot execution-style from a distance

30 cm, considered an intermediate-range wound [5]. Intermediate range was chosen to simulate executions such as the ones depicted in videos and images committed by terrorist and criminal organizations [24-25]. To simulate the execution conditions, the Synbone® spheres were anchored to a table at 112 cm (to the top of the sphere) from the ground, simulating a kneeling man of average height of 178 cm [26].

The *Synbone*® spheres were placed on a cork ring and taped with one strand of packing tape to secure them to the table Figure 2. This study, simulated executions with the victim kneeling and facing the perpetrator. The point of impact for the gunshot wound simulated entering the frontal bone at the landmark glabella and exiting the occipital bone. A shot entering the frontal bone and exiting the occipital bone was chosen for this study due to the robustness of the frontal and occipital bones and their relative thickness being close to that of the Synbone® spheres [27-28] and the fact that Synbone® being a sphere, cannot simulate the facial skeleton, which is more anatomically complex.

Data Acquisition

During the live fire iterations, a Nikon D5700, GoPro Hero, and GoPro Hero 4 were used to film the live fire execution recreations from three different angles. A Leica DM750P microscope equipped with a Leica MC170 HD 5-megapixel camera with the 4× magnification lens and Leica Live Image Builder Z software was used to capture photomicrographs of small fragments of the Synbone® spheres. A Dino-Lite Pro HR AM7013MZT(R4) 5-megapixel digital microscope and DinoCapture 2.0 software was used to analyze and take photomicrographs of the larger parts of the spheres that could not fit under the microscope.

Several macroscopic and microscopic characteristics were documented for comparative purposes. Cranial fracture types were assessed and recorded following guidelines set out by Brikley and Mckiney [29]. The following characteristics were assessed:

1. *Presence of powder tattooing and gun powder soot around the entry wound.* Power tattooing (or stippling) is the result of multiple punctate abrasions of the skin due to the impact of small fragments of gunpowder while soot deposition is the result of gases from the handgun. Both are characteristics of close range gunshots [4-5].
2. *Cranial fracture patterns (*Radius of entry and exit wound, Number or radiating and concentric fractures of entry and exit wound, minimum and maximum length or radiating and concentric fractures on entry and exit wound, number of fragments recovered on entry and exit wound).
3. *Endocranial beveling*: Endocranial beveling was measured on the endocranial surface with a flexible steel ruler and sliding calipers measuring from the point of impact to the outer margin of the endocranial beveling. A Dino-Lite Pro HR was used to take photomicrographs and to inspect the beveling microscopically.
4. *Presence of circumferential delamination*
5. *Hydraulic burst effect*: that is the damaging effects of gunshot wounds that lift portions of the cranium as described by Di Maio [5]. The presence or lack of *hydraulic burst effect* was assessed macroscopically.
6. *Presence of microfractures:* Micro-fractures in Synbone® spheres were observed from cross sections of radiating fractures emanating from the entrance wound of the spheres whenever possible using 4× magnification.
7. *Presence of Wallner lines*. These are lines generated by an acoustic wave that travels away from the point of impact [30-32] and can be used to determine crack velocity in brittle materials.

Results

Soot deposition and powder tattooing

Soot deposition was present only in one sphere and powder tattooing was present in two Synbone spheres. The .22 LR sphere showed soot deposition of 5 cm radius and powder tattooing of 9 cm radius Figure 3A. The .380 ACP sphere displayed powder tattooing of 10 cm radius but soot deposition was not present Figure 3B. Details can be found in Table 3.

Cranial Fracture Patterns

Cranial fracture types were assessed and recorded following guidelines set out by Brikley and Mckiney (2004). Table 4 and 5 illustrate fracture characteristics for entrance and exit wound respectively. Figure 4 illustrates the entry and exit wound of each round. As observed in Table 4, entrance wound radius is positively correlated with the caliber dimension as expected. The number of radiating and concentric fractures is also increasing with the caliber dimension. The .45 ACP resulted in the same number of concentric fractures but in less radiating fractures as to the entry wound compared to the smaller caliber .40 S&W. In addition, the .45 ACP resulted in the higher number of fragments at the exit wound (7) followed by the .22 LR (5). In two cases (.38 Special and .38 ACP) the fragments at the exit wound were impossible to be recovered in the shooting range due to the safety measures taken at the site.

Endocranial Beveling

The amount of endocranial beveling increased with velocity (Table 4). For example, the slowest round which was the 14.9 gm .45 ACP, with a muzzle velocity of 260 m/s had 6 mm of beveling on the endocranial surface. The 9.7 gm, .38 Special, with a muzzle velocity of 286 m/s, had 5 mm of endocranial beveling. The 6.1 gm, .380 ACP, with a muzzle velocity of 291 m/s had 6 mm of beveling on the endocranial surface. The 11.7 gm, .40 S&W with a muzzle velocity of 313 m/s had 7 mm of beveling on the endocranial surface. The 2.6 gm .22 LR with a muzzle velocity of 325 m/s had 7 mm of beveling on the endocranial surface. Last, the fastest round, the 7.5 gm, 9 x 19 mm, with a muzzle velocity of 360 m/s had 8 mm of endocranial beveling. Muzzle velocity is positively correlated with the beveling found on the endocranial exit wound of the 5 mm Synbone® spheres used in this study. The Pearson product-moment correlation coefficient test ($R=0.846$, $p<0.05$) confirms this observation.

Bullet weight, on the other hand, does not seem to correlate to the amount of endocranial beveling present in Synbone® spheres. The heaviest bullet, the 14.9 gm .45 ACP had the second smallest amount of endocranial beveling with 6 mm present (Table 1). Whereas, the 11.7 gm, .40 S&W, which is the second heaviest, had the second highest amount of endocranial beveling recorded at 7 mm.

Circumferential Delamination

Circumferential delamination was observed with the naked eye and then confirmed under magnification with a Dyno-Lite HR. The presence of this feature was observed on the .380 ACP, 9 x 19 mm, .40 S&W, and the .45 ACP. Figure 5 illustrates the circumferential delamination inflicted by the 9 x 19 mm (a) and .40 S&W (b) macroscopically, Figure 6, illustrates the circumferential delamination inflicted by .380 ACP under the Dino-lite microscopic lens.

Hydraulic burst effect

The impact of each round was recorded using two side and one front camera. Figure 7 illustrates the Hydraulic shock frame grabs from video (Supplementary material) at the time of impact for each sphere. The Hydraulic burst effect only occurred with noticeable effect on the 9 x 19 mm (8D), .40 S&W (8E), and the .45 ACP (8F).

Presence of microfractures

Synbone® spheres were examined under the Leica MC170 HD 5-megapixel camera with the 4× magnification lens and the Dino-Lite Pro HR AM7013MZT (R4) 5-megapixel digital microscope for the presence or absence of micro-fractures. No micro-fractures were observed in the six spheres examined here.

Wallner Lines Present in Synbone

The .45 ACP with the 14.9 gm round nose bullet, with a velocity of 260 m/s is the slowest velocity of this study, showed Wallner lines (Figure 8 Left). Furthermore, the 9 x 19 mm, with the 7.5 gm round nose bullet, with a velocity of 360 m/s showed an even greater increase in rippling with the ripples becoming what appears to be closer together (Figure 8 Right). It is possible that there is a direct correlation in velocity and the Wallner lines seen in Synbone® spheres.

Discussion

Animal models (mice, rats, cats etc.) have been used frequently to replicate different types of traumatic brain trauma in humans, including ballistic related brain injuries [33-35].

In addition, experimental ballistic testing has employed *Bos taurus* scapulae to substitute human crania [17] yet; the response of skeletal tissue to ballistic impacts is highly affected by the anatomical differences between animal surrogates and human crania [36]. As an alternative, PBS spheres are being used at an increased rate, as they appear to be a good proxy to human crania macroscopically (they are morphologically more similar to human cranial than animals) and their use alleviates the multitude of ethical problems associated with using animal bone and human cadaveric material [16, 36] On the other hand, PBS spheres are uniform in thickness allowing ballistic testing to reproduce with little variation unlike human crania, which have varying thicknesses and morphological differences between individuals [37]. Hence, they can be safely used to simulate the biggest portion of the cranial vault, but are not appropriate for the facial skeleton, which exhibits considerable anatomical complexity.

This study seeks to investigate the differences in trauma patterns associated with different handguns and calibers, in a series of experiments, using artificial proxies for human crania. The experiments maintained several controlled variables (same "anatomical region", distance from the target, same person taking the shot) in an effort to reduce bias with the observable trauma patterns. We tested six different handgun calibers (.22 LR, .38 Special, .380 ACP, 9 x 19 mm, .40 Smith & Wesson (S&W), and .45 ACP. All rounds fired in this study are considered medium velocity; meaning between 152 m/s to 457 m/s [21-23]. Seven characteristics (see material and methods) were recorded and compared between the different rounds with the objective to detect similarities and differences that could help in their differentiation in future investigations of ballistic injuries. These are thoroughly discussed below.

Powder tattooing is one of the hallmarks of intermediate-range gunshot wounds [3-5, 38]. Spitz [4] notes that for most handguns residues can be detected on the skin at firing distances of 46-61 cm. We fired all rounds from 30 cm distance and observed powder tattooing in only two cases. Soot seen on the .22 LR sphere (Figure 3) is a common occurrence with rimfire cartridges [4-5,38] and is in line with what we would have expected following Spitz's thresholds. The maximum diameter of the powder tattooing was 9 cm (Table 3). In contrast, the .380 ACP sphere showed powder tattooing with maximum diameter of 10 cm (Figure 3) but no signs of soot were noted These observations reinforce

Spitz's statement that "the approximate distance from which a close-range shot was fired can be evaluated only by test firing the particular weapon, using the same type of ammunition as that used in the shooting case under consideration". Consequently, based on our study, one could devise that shots fired at a distance ≥ 30 cm with 9 x 19 mm, .40 S&W, or .45 ACP would not have resulted in any soot deposition nor power tattooing. Yet, different ammunition may yield different results for this as manufactures use different powder types.

According to our results, entrance wound radius is positively correlated with the caliber dimension as expected. The number of radiating and concentric fractures is also increasing with the caliber dimension. The .45 ACP seems to be less destructive as to the entry wound compared to the smaller caliber .40 S&W. In all cases, the bullet exited the sphere. The exit wound presents a similar correlation between the number of radiating and concentric fractures and the caliber size.

The amount of endocranial beveling increased with velocity. The bullet weight, conversely, does not seem to be suggestive of the amount of endocranial beveling present in Synbone® spheres. Visual comparisons of endocranial beveling of the entrance wounds between Synbone® ballistic spheres and human crania resulted in many similarities. The Synbone® sphere shot with .22 LR had no radiating or concentric fractures but presented endocranial beveling and matched well, visually, with a documented forensic case (Figure 9) of a GSW from a .22 LR at intermediate range (Source: P. Mylonakis, Forensic Pathologist, Medical Examiner's Office of Thessaloniki, Greece). On the other hand, the Synbone® sphere shot with .45 ACP showed radiating fractures with endocranial beveling and had impressive similarities to a GSW (Figure 10) with .45 ACP from intermediate range (Source: P. Mylonakis, Forensic Pathologist, Medical Examiner's Office of Thessaloniki, Greece).

Circumferential delamination was also recorded in our experiments (Figure 5-6). This feature is indicative of FMJ rounds in human crania as described by Kimmerle and Baraybar [9]. The authors describe a case of close-range extrajudicial execution with a 9 x 19 mm with FMJ rounds which resulted in circumferential delamination on the entrance wound (occipital bone). Out of the six spheres shot in our study, four exhibited circumferential delamination. More specifically, all the Synbone® shot with FMJ rounds displayed circumferential delamination quite well. Hence, the preliminary findings of this

study suggest that circumferential delamination is expected to be found in FMJ rounds shot from 30 cm distance on Synbone® spheres.

The study also explored the Hydraulic burst effect; that is the damaging effects of gunshot wounds that lift portions of the cranium as described by Di Maio [5]. Hollow organs, with a liquid filled bladder like a human head (brain material is classified a liquid), cause an immense amount of pressure inside the cranium [39]. If the projectile has enough energy, it will cause the human head to rupture [7, 9, 39]. However, not every bullet wound to the head will cause the hydraulic explosive effect. The ballistics of the bullet and the pressure applied to the brain are the main factors causing hydraulic bursting. The higher the velocity of the round and the size of the leading face of the bullet will result in higher pressures being produced in the cranium [7, 40, 41]. In our study, we recorded the existence of the hydrostatic effect in three rounds. The largest round shot in our study was the .45 ACP (11.5 mm) which also had the most hydrostatic shock (Figure 7f). We compared our results with the ballistic study of Appleby-Thomas et al. [42]. The amount of hydraulic burst on our three rounds was more extensive and could be attributed to the projectile type, as Appleby-Thomas et al. [42] used 12 mm stainless steel spheres, which do not deform and have a large leading face.

Micro-fractures in bone can be seen in velocities as low as 60 m/s [43]. With high-velocity rounds -greater than 457 m/s it has been shown that velocities and round types can be identified by individual fracture patterns [17]. However, there is a lack of data on medium velocity rounds (such as those used in this study) on whether or not they produce microscopic fracture patterns that can be used to identify velocities or round type. These micro-fractures can be used to discern the direction of travel as the micro-fractures travel away from the point of impact [17, 43]. Nevertheless, no micro-fractures were observed in this current study. Lack of observable micro-fractures seems to corroborate the findings of Smith et al. [16] who agree PBS spheres do not have the same properties of cortical bone, which micro-fractures can cause lateral deflection of portions of cortex, directional cortical bending, and delamination.

Macroscopically, Synbone® performs well as a proxy to crania. Entrance wounds have a similar appearance, radiating, and concentric fracturing are consistent with

caliber, and circumferential delamination is expressed well with the FMJ rounds used in this study. Hydraulic shock and endocranial beveling are also consistent with caliber, velocity, and size of the leading face of the bullet. The exit wounds, however, tend to be much larger than real examples as pointed out by Smith et al. [16] and confirmed by this study. The observations made by Smith et al. [16] about Synbone® not responding to ballistic trauma the same way bone does, microscopically, is founded. It is evident under the microscope; Synbone® does not have the same microstructure and flexibility. Synbone® is more brittle than bone, as seen with what is thought to be Wallner lines. Further research is needed to confirm and add to the preliminary observations of this study. There are some intriguing prospects for future ballistic testing with Synbone. Future work should include larger number of experiments and should also focus on ballistic testing of different anatomical regions including the face and neck, taking into account factors such as the presence of hair and/or different head wear, with a variety of projectiles and other weapons (e.g. blunt/sharp objects) in an effort to establish clear-cut diagnostic criteria for weapon identification using artificial cranial proxies.

Acknowledgments

Funding for this study project was provided by the University of Edinburgh. We thank Emmanouil Kouridakis from the National shooting range in Chania, Crete, for providing the pistols, ammunition, and time as Range Safety Officer. A gigantic thank you to the Greek National Shooting Club, Chania, for allowing us unlimited access to the private pistol range, providing the table on which we conducted the shooting, and the necessary protective equipment for the observers and shooter. Lastly, we would like to thank Jessica Schalburg and CK Franklin for the help with photographs and preparations of the Synbone® spheres. Finally, we would like to thank the two anonymous reviewers for their insightful comments. The experimental study described in this paper was conducted during the course of a Forensic Anthropology MSc undertaken by the author, Seth C. Taylor, at the University of Edinburgh in 2015/2016. The experiments took place during the 2016 Crete field school.

References

1. E. Grinshteyn, D. Hemenway, Violent Death Rates: The US Compared with Other High-income OECD Countries, 2010, Am J Med 129 (2016) 266-273
2. N. Duquet, M. Van Alstein, 2015 Firearms and Violent Deaths in Europe. The Flemish Peace Institute
3. A.R. Moritz, The Pathology of Trauma, 2nd edition Philadelphia; 1954.
4. W.U. Spitz. Injury by gunfire in *Spitz and Fisher's Medicolegal Investigation of Death: Guidelines for the Application of Pathology to Crime Investigation*. Spitz, W.U. and Spitz, D.J., editors, 4rth edition, Charles C Thomas Publisher 2006 pp. 607-747
5. V.J.M., Di Maio, 2015. *An Introduction to the Classification of Gunshot Wounds*: *Gunshot Wound Practical Aspects of Firearm, Ballistics and Forensic Technique. 3rd edition. CRC Press*.
6. G.O. Hart, Fracture pattern interpretation in the skull: differentiating blunt force from ballistics trauma using concentric fractures. J Forensic Sci, 50(2005), 1276-81.
7. B.P. Kneubuehl. Wound Ballistics: Basics and Applications, © Springer-Verlag Berlin Heidelberg 2011
8. B. Madea, M. Staak. Determination of the sequence of gunshot wounds of the skull. *J Forensic Sci Soc.* 28(1988):321-8.
9. E.H. Kimmerle, and J.P. Baraybar, Skeletal Trauma: Identification of Injuries Resulting from Human Rights Abuse and Armed Conflict. CRC Press, 2008.
10. E.F. Kranioti. Forensic investigation of death due to blunt force trauma: current best practice. Research and Reports in Forensic Medical Science. 5 (2015a) 25-37.
11. M.J. Thali, B.P. Kneubuehl, U. Zollinger and R. Dirnhofer. The "skin–skull–brain model": a new instrument for the study of gunshot effects. *Forensic Sci Int*, *125* (202) 178-189.
12. M.J. Thali, B.P. Kneubuehl, U. Zollinger and R. Dirnhofer. 2002. A study of the morphology of gunshot entrance wounds, in connection with their dynamic creation, utilizing the "skin–skull–brain model". *Forensic Sci Int 125* (2002) 190-194.

13. M.J. Thali, B.P. Kneubuehl, U. Zollinger and R. Dirnhofer. 2002. The dynamic development of the muzzle imprint by contact gunshot: high-speed documentation utilizing the "skin–skull–brain model". *Forensic Sci Int 127* (2002) 168-173.
14. E.F. Kranioti. Investigation of cranial blunt force trauma using SYNBONE artificial spheres. Winter meeting of the British Association for Forensic medicine. Edinburgh November 21st, 2015b.
15. A. Ruchonnet, H. Langstaff, M. Diehl, Y-H Tang, E. F. Kranioti Cranial Blunt Force Trauma on Resistance- Free Individuals vs Individuals Resting on a Solid Surface. Annual conference of the British Association for Human Identification, Manchester, 11th-13th December 2015.
16. M.J. Smith, James, S., Pover, T., Ball, N., Barnetson, V., Foster, B., Guy, C., Rickman, J. and Walton, V., 2015. Fantastic plastic? Experimental evaluation of polyurethane bone substitutes as proxies for human bone in trauma simulations. *Legal Medicine*, *17*(5), pp.427-435.
17. J.M. Rickman, M.J. Smith. Scanning Electron Microscope Analysis of Gunshot Defects to Bone: An Underutilized Source of Information on Ballistic Trauma. J Forensic Sci, 59 (2014) 1473-1486.
18. K. Hwang, J.H. Kim, J.H., S.H. Baik, 1999. The thickness of the skull in Korean adults. *J Craniof Surg*, *10* (1999) 395-399.
19. H. Jung, H.J. Kim, Kim, D.O., Hong, S.I., Jeong, H.K., Kim, K.D., Kim, Y., Yoo, S. and Yoo, H., 2002. Quantitative analysis of three-dimensional rendered imaging of the human skull acquired from multi-detector row computed tomography. *Journal of Digital Imaging*, *15*(4), pp.232-239.
20. Synbone® Company website: https://www.Synbone®.ch/wEnglish/index.php and https://www.Synbone®.ch/wEnglish/catalogue/index.php?navanchor=1010042. Last accessed on the 6th of June 2017.
21. D.F. Huelke, J.H. Darling 1964. Bone fractures produced by bullets. J *Forensic Sci*, *9* (1964) 461.
22. D.F. Huelke, L.J. Buege, J.H. Harger Bone fractures produced by high velocity impacts. *Am J Anatomy*, *120* (1967), pp.123-131.
23. M. Bussard, 2014. *5th Edition Ammo Encyclopedia: For all Rimfire and Centerfire*

Cartridges, Plus Shotshells! Blue Book Publications.

24. C. Charlton, 2015. Father of 'spy' said to have been shot by child in ISIS video says his son was duped into JOINING Islamic State... then killed for trying to return home [online]. Mail Online. Available from: http://www.dailymail.co.uk/news/article-2988352/islamic-state-s- propaganda-arm-announces-broadcast-execution-israeli-spy-captured-syria-year.html [Accessed 25 Jun 2016].
25. ChingaOne, 2016. Does latest ISIS video REALLY show a child shooting a man dead? Boy's face cannot be seen when 'Israeli spy' is killed... and gunman's hand looks to be a man's, not a ten-year-old's [online]. ChingaOne. Available from: http://www.chingaone.com/2015/03/does-latest-isis-video-really-show.html [Accessed 25 Jun 2016].
26. D. Kahneman, A. Tversky, Subjective probability: A judgment of representativeness. *Cognitive Psychology*, *3* (1972) 430-454
27. K. Hwang, J.H. Kim, S.H. Baik, The thickness of the skull in Korean adults. *Journal of Craniofacial Surgery*, *10* (1999) 395-399.
28. N. Lynnerup, J.G. Astrup, B. Sejrsen, Thickness of the human cranial diploe in relation to age, sex and general body build. *Head & Face Medicine*, *1* (2005) 1.
29. M. Brickley, J.I. McKinley, 2004. *Guidelines to the Standards for Recording Human Remains*. Institute of Field Archaeologists Technical Paper No. 7, BABAO/IFA. *Reading*.
30. C. Kocer, R.E. Collins, Angle of Hertzian cone cracks. *Journal of the American Ceramic Society*, *81* (1998) 1736-1742.
31. A. Rabinovitch, V. Frid, D. Bahat Wallner lines revisited. *Journal of Applied Physics*, *99* (2006), pp. 1-3.
32. R.L. Narayan, P. Tandaiya, R. Narasimhan, U. Ramamurty, Wallner lines, crack velocity and mechanisms of crack nucleation and growth in a brittle bulk metallic glass. *Acta Materialia*, *80* (2014) 407-420.
33. Carey ME, Sarna GS, Farrell JB, Happel LT. Experimental missile wound to the brain. J Neurosurg. 71 (1989) 754–764
34. A.J. Williams, J.A. Hartings, X.C. Lu, M.L. Rolli, F.C. Tortella Penetrating ballistic-like brain injury in the rat: differential time courses of hemorrhage, cell death,

inflammation, and remote degeneration. J Neurotrauma. 23 (2006)1828–1846

35. A.J. Williams, G.S. Ling, F.C. Tortella, Severity level and injury track determine outcome following a penetrating ballistic-like brain injury in the rat. Neurosci Lett. 408 (2006)183–188.
36. C. Humphrey, J. Kumaratilake Ballistics and anatomical modelling – a review. Leg Med 23 (2016) 21–29
37. T.W. Fenton, V.H. Stefan, L.A. Wood, N.J. Sauer, Symmetrical fracturing of the skull from midline contact gunshot wounds: reconstruction of individual death histories from skeletonized human remains. *J Forensic Sci*, *50* (2005) 8-12.
38. J.A. Prahlow, R.W. Byard, 2011. *Atlas of Forensic Pathology: for Police, Forensic Scientists, Attorneys, and Death Investigators*. Springer Science & Business Media.
39. K.G. Sellier, and B.P. Kneubuehl, 1994. Wound Ballistics and the Scientific Background. Elsevier Health Sciences.
40. E.N. Harvey, J.H. McMillen, An experimental study of shock waves resulting from the impact of high velocity missiles on animal tissues. The Journal of Experimental Medicine, 85(1947) .321-328.
41. F.P. Watkins, B.P. Pearce, M.C, Stainer, 1988. Physical effects of the penetration of head simulants by steel spheres. Journal of Trauma and Acute Care Surgery, 28(1), pp. S40-S54.
42. G.J. Appleby-Thomas, D.C. Wood, A. Hameed, J. Painter, V. Le-Seelleur, B.C. Fitzmaurice, Investigation of the high-strain rate (shock and ballistic) response of the elastomeric tissue simulant Perma-Gel®. *International Journal of Impact Engineering*, *94* (2016) 74-82.
43. D.C. Kieser, R. Riddell, J.A. Kieser, J.C. Theis, M.V. Swain, Bone micro-fracture observations from direct impact of slow velocity projectiles. *Journal of Archives in Military Medicine*, *2*(2014).

Figure 1. Ammunition used in this study (left to right): .22 LR, .38 Special, .380 ACP, 9 x 19 mm, .40 S&W, and .45 ACP (Photo Steven Portz, Black Flag Firearms LLC).

Figure 2. Experimental setting: The Synbone® spheres were placed on a cork ring and taped with one strand of packing tape to secure them to the table.

Figure 3. The .22 LR (A) round resulted in powder soot with 5 cm maximum dimeter and 9 cm stippling on the Synbone sphere. The .380 ACP (B)round produced stippling with maximum diameter of 10cm with absence of powder soot.

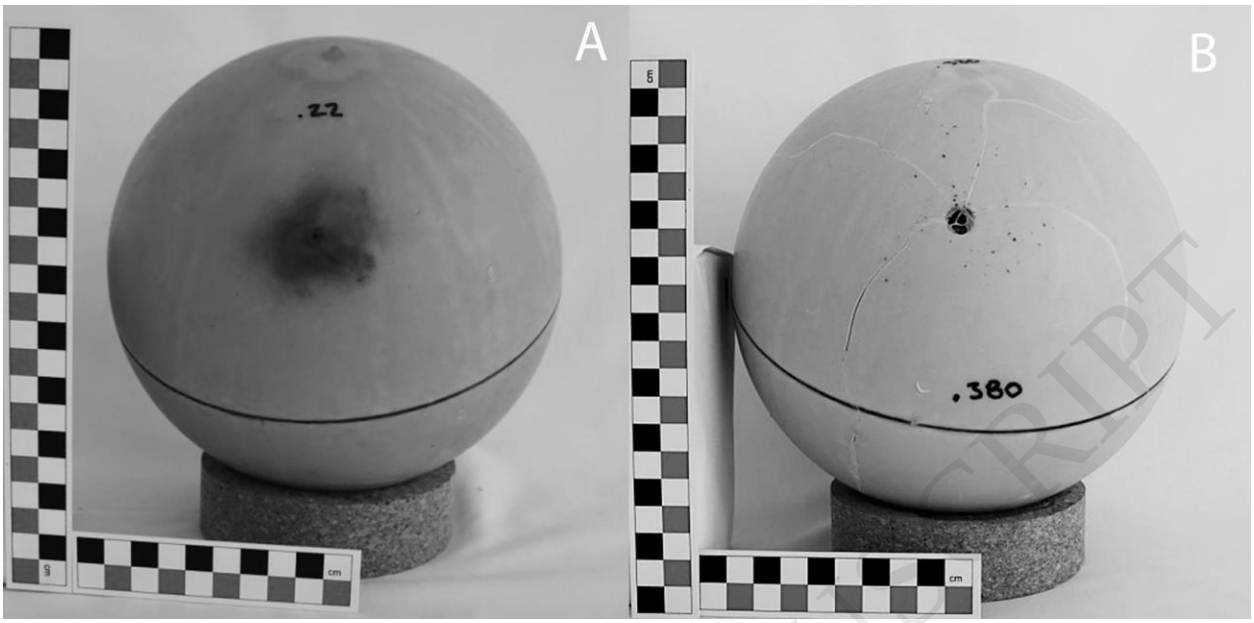

Figure 4. Entry and exit wound of each round respectively: .22 LR (a,b), .38 Special (c,d), .380 ACP (e,f), 9 x 19 mm (g,h), .40 S&W (i, j), and .45 ACP (k,l).

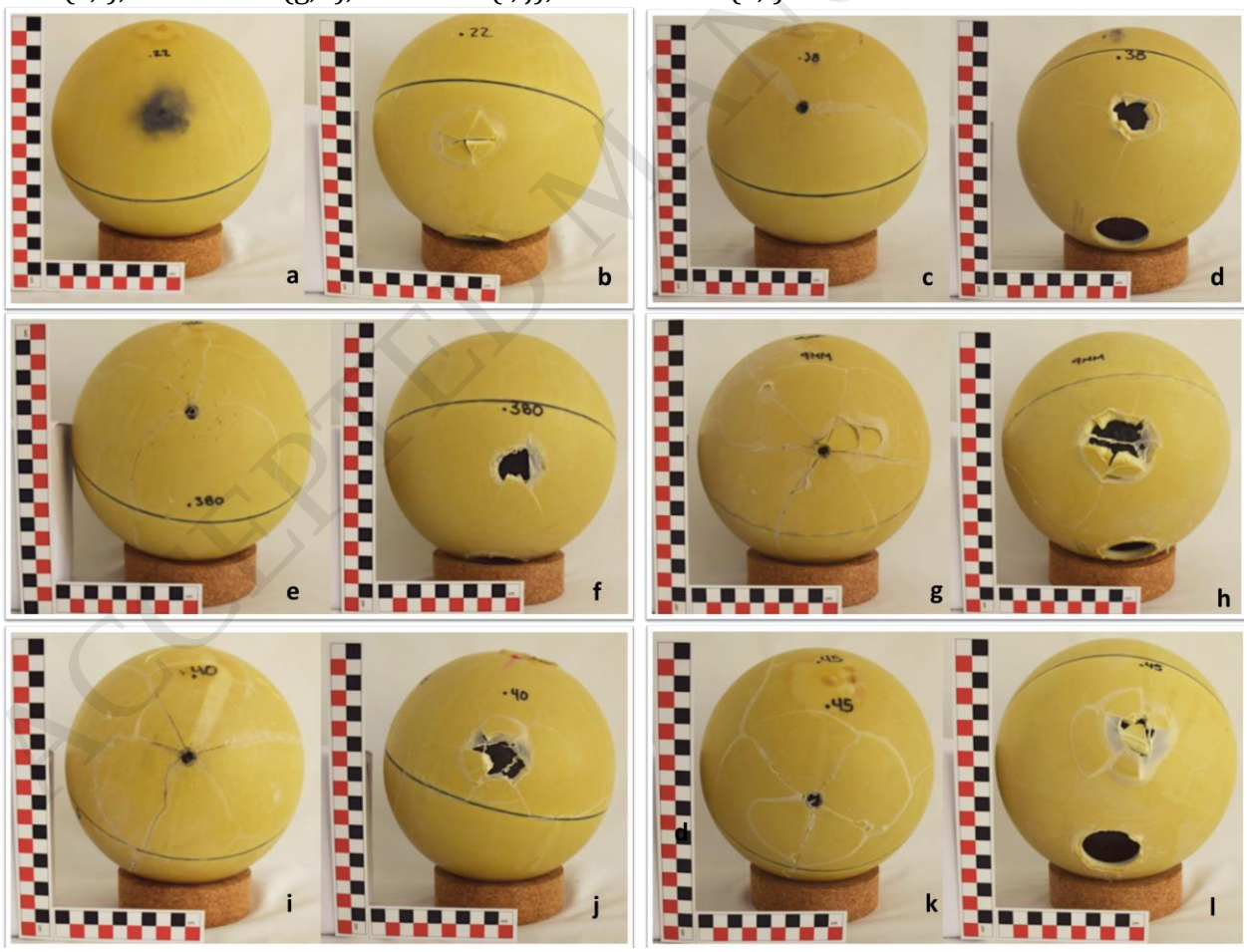

Figure 5. Circumferential delamination inflicted by the 9 x 19 mm (a) and .40 S&W (b).

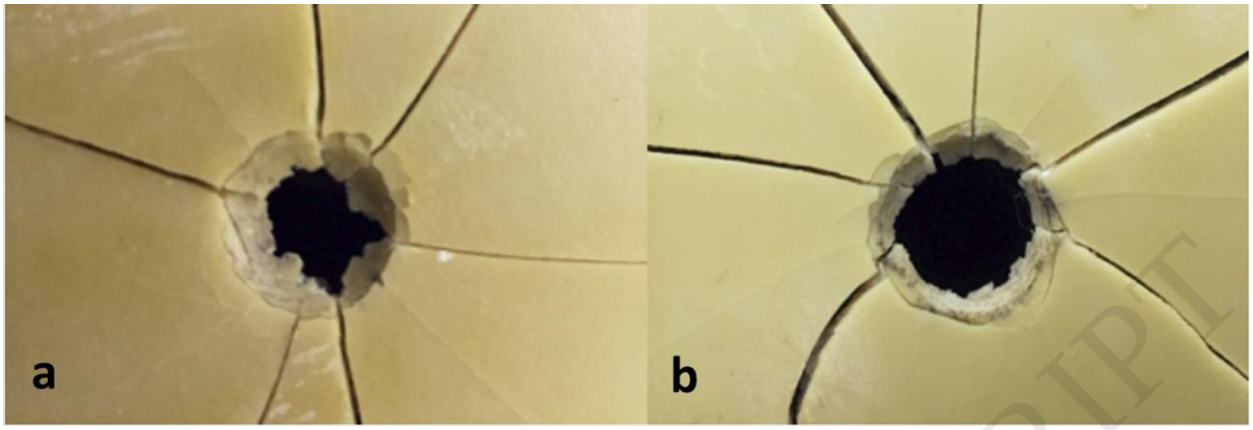

Figure 6. Circumferential delamination inflicted by the .380 ACP.

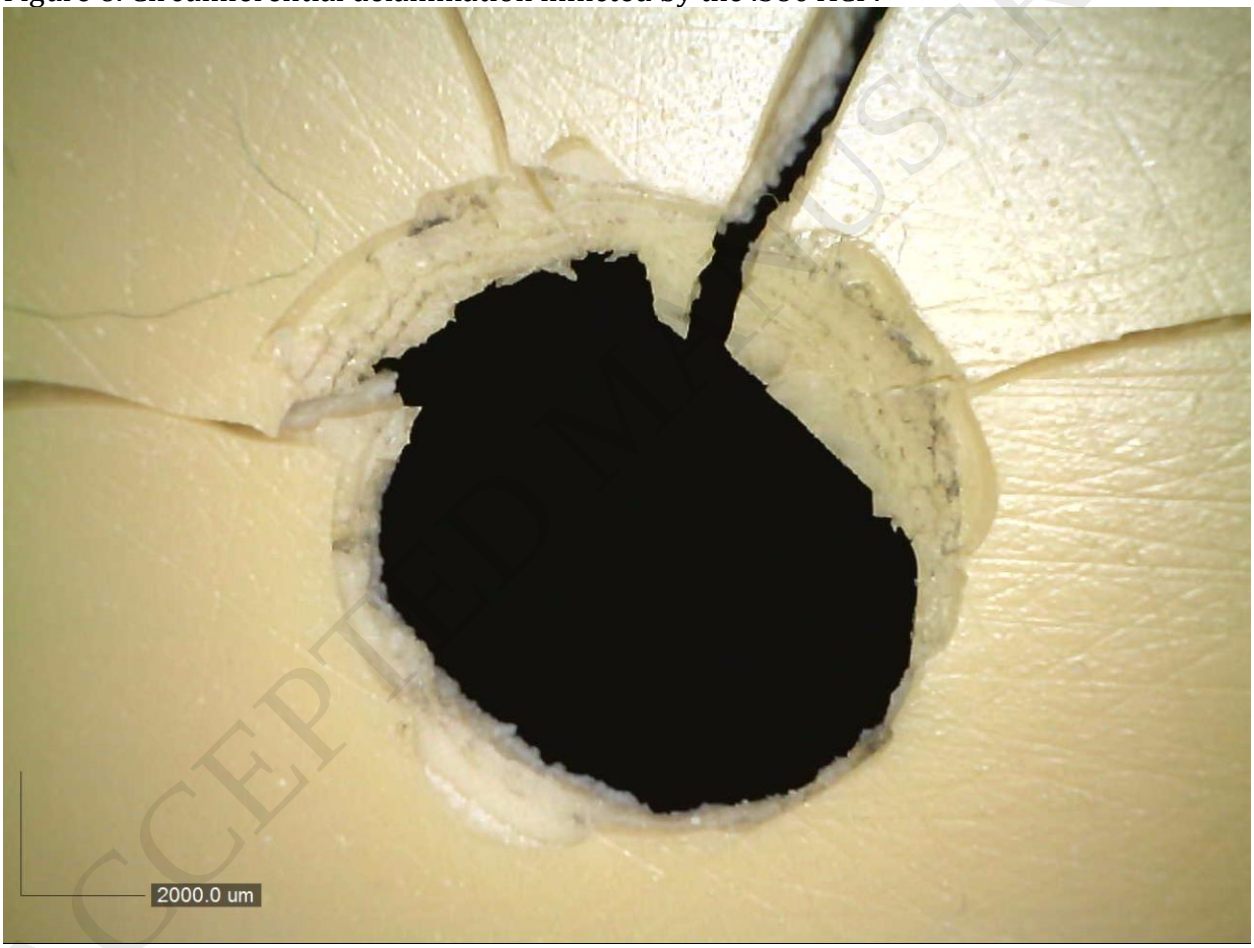

Figure 7. Hydraulic burst frame grabs from video at the time of impact for each round: .22 LR (A), .38 Special (B), .380 ACP (C), 9 x 19 mm (D), .40 S&W (E), and .45 ACP (F). The Hydraulic burst effect only occurred with noticeable effect on the three last rounds (D-F).

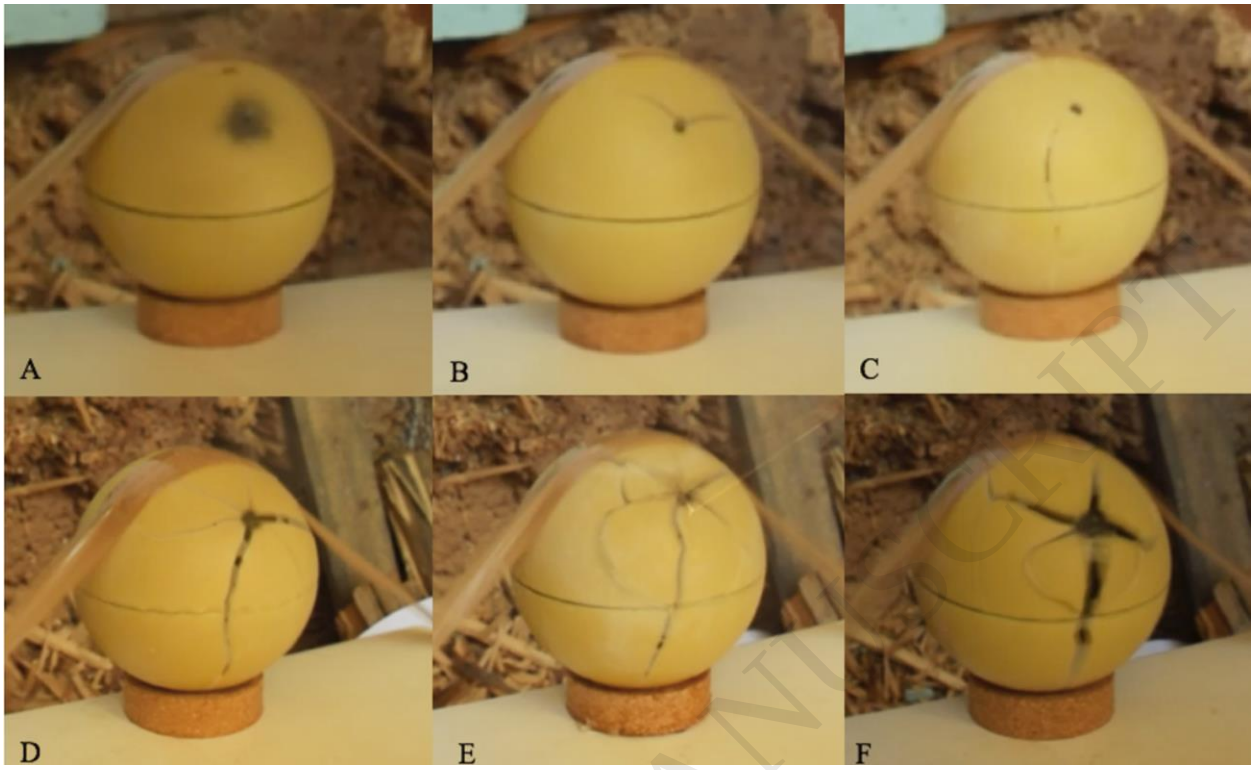

Figure 8. Presence of Wallner lines provoked by the .45 ACP (left) and the 9 x 19 mm (right).

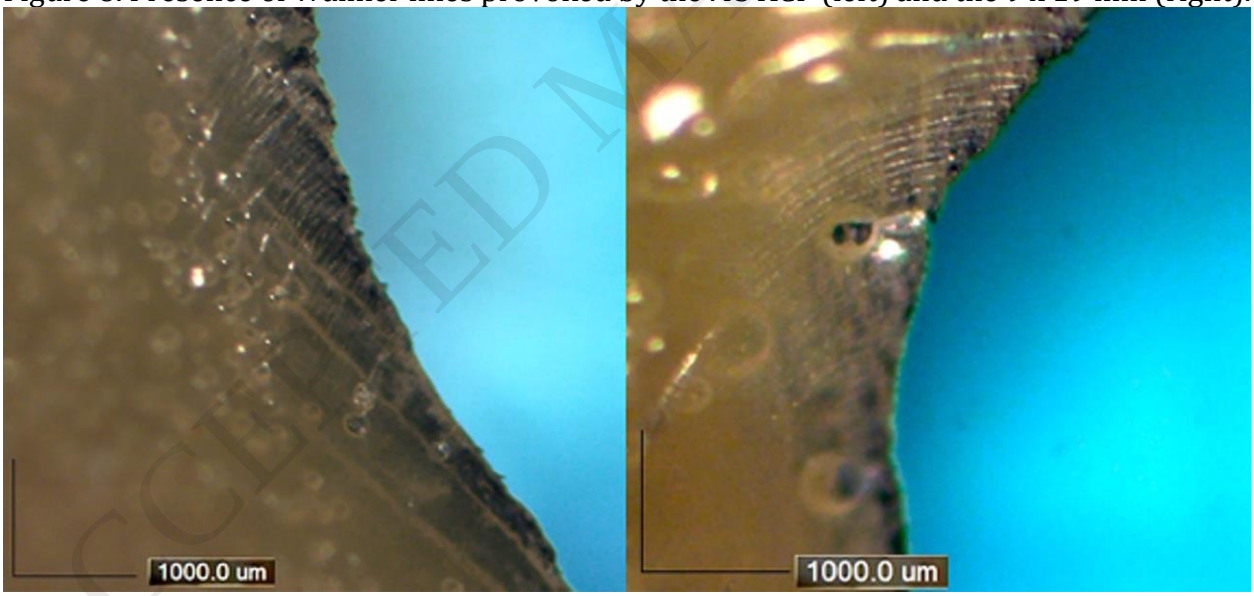

Figure 9. The Synbone® sphere shot with .22 LR had no radiating or concentric fractures (a) but presented endocranial beveling (b) and matched well, visually, with a documented forensic case of a GSW from a .22 LR at intermediate range (c,d). Source: P. Mylonakis, Forensic Pathologist, Medical Examiner's Office of Thessaloniki, Greece.

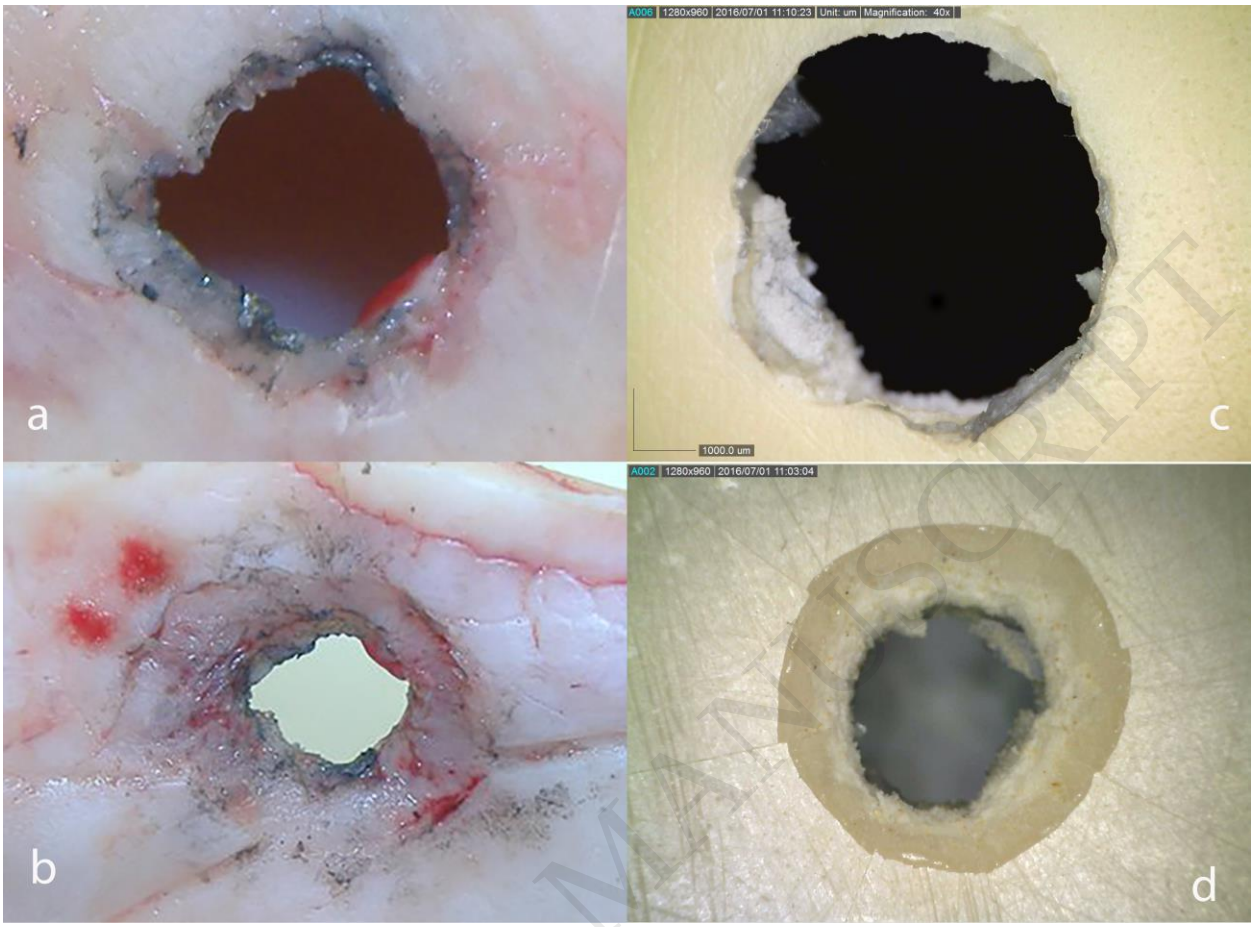

Figure 10. The Synbone® sphere shot with .45 ACP showed radiating fractures with endocranial beveling (a) and had impressive similarities to a GSW with .45 ACP from intermediate range (b). Source: P. Mylonakis, Forensic Pathologist, Medical Examiner's Office of Thessaloniki, Greece.

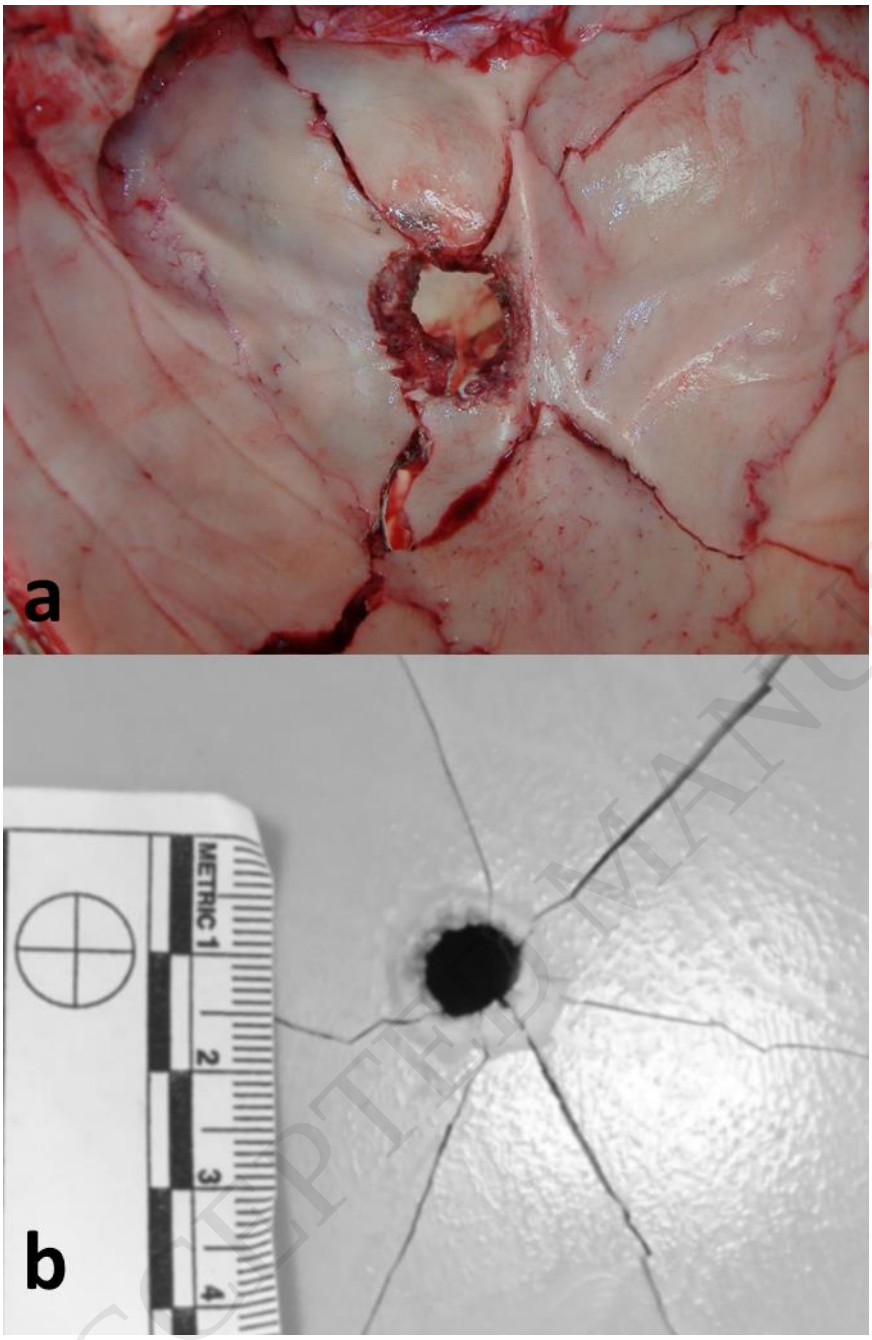

Table 1. Sellier & Bellot, ammunition used for the study.

Caliber	**Bullet weight**	**Muzzle velocity**	**Muzzle energy (Joules)**
.22 LR	2.56 gm	325 m/s	135
.38 Special	9.7 gm	286 m/s	419
.380 ACP	6.1 gm	291 m/s	254
9 x 19 mm	7.5 gm	360 m/s	518
.40 S&W	11.7 gm	313 m/s	524
.45 ACP	15 gm	260 m/s	504

Adopted from Sellier and Bellot (2016)

Table 2. Presence and size of soot and powder tattooing.

Cartridge	Soot	Powder tattooing
.22 Long Rifle	5cm maximum diameter	9 cm maximum diameter
.38 Special	-	-
.380 ACP	-	10 cm maximum diameter
9 x19 mm	-	-
.40 S&W	-	-
.45 ACP	-	-

Table 3. Entrance wound assessments.

Caliber	**Entrance wound diameter (mm)**	**Radiating fractures (#)**	**Concentric fractures (#)**	**Radiating fracture maximum /minimum length (cm)**	**Concentric fracture maximum /minimum length (cm)**	**Fragments recovered (#)**	Endocranial beveling
.22 Long Rifle	6	0	0	0	0	0	5 mm
.38 Special	9.5	2	0	21 / 20	0	0	6 mm
.380 ACP	10	4	1	21 / 14	5.5 / -	0	6 mm
9 x 19 mm	10	6	2	29 / 18	12/7	4	7 mm
.40 S&W	12	6	5	26.5 / 13	9 / 2	4	7 mm
.45 ACP	13	4	5	20 / 4.5	11.2 / 2.5	3	8 mm

Table 4. Exit wound assessments.

Caliber	**Exit wound diameter (cm)**	**Radiating fractures (#)**	**Concentric fractures (#)**	**Radiating fracture maximum/ minimum length (cm)**	**Concentric fracture maximum /minimum length (cm)**	**Fragments recovered (#)**
.22 Long Rifle	3.2 x 3.4	5	0	2.3 / 1	- /-	5
.38 Special	2.3 x 2.8	5	0	6.5 / 3	- / -	NR
.380 ACP	2.2 x 3.6	6	0	5.5 / 2.5	- /-	NR
9 x 19 mm	4.6 x 4.8	5	0	9.5 / 2	- /-	3
.40 S&W	5.3 x 3.9	7	1	5.6 / 3	11 / -	3
.45 ACP	5.7 x 6.6	4	2	3 / 2	2 / -	7

NR=not recovered